THE BELTRAMI GEOMETRICAL FRAMEWORK OF COLOR IMAGE PROCESSING

Nir Sochen and Yehoshua Y. Zeevi

Department of Electrical Engineering
Technion- Israel Institute of Technology
Technion City, Haifa 32000, Israel
sochen,zeevi@ee.technion.ac.il

ABSTRACT

The Beltrami geometrical framework for scale-space flows is generalized to nontrivial color space geometries and implemented in analysis and processing of color images. We demonstrate how various models of color perception, interpreted as geometries of the color space, result in different enhanced processing schemes.

1. INTRODUCTION

The relationship between processing of color images and color perception is a longstanding issue that had attracted variety of approaches and techniques. To start with, in dealing with color images one has to determine and define the proper space for their representation. Traditionally, the R, G, B coordinates have been transformed into one achromatic coordinate and two chromatic coordinates not necessarily related to the neurophysiology and perception of color [1]. Further, the representations have been considered, in most cases, in relation to the chromatic aspects of the image space separately from the spatial coordinates. As far as the spatial coordinates are concerned, several recent studies have demonstrated the advantages inherent in partial differential techniques adopted from heat-like and diffusion-like models [10].

We present and implement a method that employs the recently proposed geometric Beltrami framework for nonlinear scale-space methods [10]. According to this framework, an image is treated as an embedding of a manifold in a higher dimensional spatial-feature manifold. The embedding manifold is a hybrid space that includes spatial coordinates as well as feature coordinates. The features may include, apart from intensity and color, elements of the intensity jet bundle (basically derivatives of the intensity), wavelet parameters like typical local size and orientation [3], statistical characteristics [15] and others. The choice of the appropriate embedding space depends on the class of images to be processed and the nature of the task. We encode knowledge about the task and the nature of the feature space in the geometry of the embedding space.

A grey level image is considered in this framework as a two-dimensional surface (i.e. the graph of $I(x,y)$) **embedded** in the three-dimensional space whose coordinates are (x,y,I). A color image is accordingly considered as a two-dimensional surface **embedded** in the five-dimensional space whose coordinates are (x,y,U_1,U_2,U_3) where the coordinates (U_1,U_2,U_3) are color coordinates (for example $(U_1,U_2,U_3)=(R,G,B)$). Texture can be treated as a 4-dimensional space embedded in $\mathbb{R}^6$ [3].

It was suggested [10] that the nonlinear scale space may be treated as a gradient descent with respect to a functional integral that depends on the geometry (i.e. the metric) of the image surface, as well as on the embedding and the geometry of the embedding space. In the examples treated in the past, it was assumed that the embedding space is Euclidean and that the system of coordinates that describes it, is Cartesian [10], [3]. In fact, the geometry of the embedding space is flexible and can be determined according to an a priory knowledge about the class of images to be processed and the high level task that one has in mind [11]. We view the geometry of the embedding space as the interface between the high-level task, the a priory knowledge and the low-level process to be implemented.

We treat in this study color images. Textured color images with a non-Euclidean embedding space are treated elsewhere [11]. Color space and its perception has fascinated researchers for over a century. It is natural, from our viewpoint, to apply our framework for this class of color images since the knowledge accumulated along the years is organized and encoded in the geometry of the color space. This form is especially convenient and ready to use in the Beltrami framework.

This research has been supported in part by the Ollendorff Center, the Fund for Promotion of Research at the Technion, and by the Ministry of Science Vision Platform Project.

2. COLOR SPACE GEOMETRY

Two issues should be addressed in the process of evaluating the geometry of the color space. The first relates to the variables (or coordinates), and the second to its geometry. Attempts to describe the color perception geometry go back more than a hundred years. Helmholtz [2] was the first to define a 'line element' (arc-length) in color space. He first used a Euclidean R, G, B space defined by the arc-length:

$$ds^2 = (c_r d\log R)^2 + (c_g d\log G)^2 + (c_b d\log B)^2. \quad (1)$$

His first model failed to represent empirical data of human color perception. Schrödinger [8] modified the Helmholtz model by introducing the arc-length:

$$ds^2 = \frac{1}{L}\left(\frac{c_r(dR)^2}{R} + \frac{c_g(dG)^2}{G} + \frac{c_b(dB)^2}{B}\right), \quad (2)$$

where $L = c_r R + c_g G + c_b B$ and c_r, c_g, c_b are constants. Schrödinger's model was later found to be inconsistent with findings on threshold data of color discrimination.

Koenderink et al. [4] generalized these line elements with a family of metrics

$$ds^2 = (L)^{\alpha-2}\left(\frac{c_r(dR)^2}{R^\alpha} + \frac{c_g(dG)^2}{G^\alpha} + \frac{c_b(dB)^2}{B^\alpha}\right), \quad (3)$$

where different values of α correspond to different models: $\alpha = 2$ is the Helmholtz model, $\alpha = 1$ is Schrödinger's. Koenderink et al. [4] studied the $\alpha = 0$ case.

Stiles et al. [13] advocated another generalization of the Helmholtz line element

$$ds^2 = (c_r d\log(R'))^2 + (c_g d\log(G'))^2 + (c_b d\log(B'))^2, \quad (4)$$

where $R' = aR + b$ with a, b constants, and similarly for G' and B'. Other analytical attempts culminated in the Vos-Walraven line element which is much more involved and will not be treated here.

MacAdams constructed an empirical line element based on direct psychophysical experiments. His result can be given in tables and graphs only. The theoretical challenge is the construction of an analytical line element that is capable of explaining all the features of the color perception space that were found in MacAdams experimental data.

3. THE GEOMETRIC BELTRAMI FRAMEWORK

This framework is based on geometrical ideas borrowed from general relativity and high energy physics. The essence of the method is summarized in two aspects of the formalism:

a) A two-dimensional image is a Riemannian surface embedded in a higher dimensional Riemannian manifold which is called the spatial-feature manifold. Let introduce on the nonlinear surface a local coordinate system (σ^1, σ^2). The embedding of this surface in, say, a three-dimensional space with coordinates (X^1, X^2, X^3), is done by specifying, for each point of the surface, the three-dimensional coordinates, namely:

$$(X^1(\sigma^1,\sigma^2), X^2(\sigma^1,\sigma^2), X^3(\sigma^1,\sigma^2)). \quad (5)$$

We say that X is a map that embeds the surface Σ with metric $(g_{\mu\nu})$ in a higher dimensional Riemannian manifold M with metric (h_{ij}). The local metric $(g_{\mu\nu})$ is given as the *induced metric* in terms of the embedding map and the embedding space metric by

$$g_{\mu\nu}(\sigma^1,\sigma^2) = \sum_{i,j=1}^{\dim M} h_{ij}(\mathbf{X})\partial_\mu X^i \partial_\nu X^j, \quad (6)$$

where $\partial_\mu X^i \equiv \partial X^i(\sigma^1,\sigma^2)/\partial\sigma^\mu$. In the sequel we will use Einstein convention and drop the summation sign.

We introduce a one-parameter family of embedded images $(X^i(\sigma^1,\sigma^2;t))_{i=1}^3$, where t is the evolution independent variable, called the scale or "time". This parameter determines the degree of blurring or denoising of the image.

b) From a geometrical viewpoint, this family of embedded images describes a flow of a two-dimensional surface within a higher dimensional space. The dynamics of the surface along the flow are governed by nonlinear heat equation applied to this one parameter family of images. The equation is derived as a gradient descent of a functional that weight embedding maps in a geometrical manner.

The functional in question, $S[\cdot,\cdot,\cdot]$, depends on *both* the image manifold and the embedding space. Denoting by $(\Sigma, (g_{\mu\nu}))$ the image manifold and its metric and by $(M, (h_{ij}))$ the spatial-feature manifold and its metric, the map $\mathbf{X} : \Sigma \to M$ has the following weight [7]:

$$S[X^i, g_{\mu\nu}, h_{ij}] = \int d\sigma^1 d\sigma^2 \sqrt{g} g^{\mu\nu} \partial_\mu X^i \partial_\nu X^j h_{ij}(\mathbf{X}), \quad (7)$$

where g is the determinant of the image metric, $g^{\mu\nu}$ denotes the inverse of the image metric, $\mu, \nu = 1, 2$, and $i, j = 1, \ldots, \dim M$.

The Polyakov action is the generalization of the L_2 norm from Euclidean space to curved spaces. Here, $d\sigma^1 d\sigma^2 \sqrt{g}$ is the area element of Σ and $g^{\mu\nu}\partial_\mu X^i \partial_\nu X^j h_{ij}(\mathbf{X})$ is the generalization of $|\nabla I|^2$ to maps between non-Euclidean manifolds. Note that the volume element as well as the rest of the expression is invariant under reparameterization, that is, $\sigma^\mu \to \tilde{\sigma}^\mu(\sigma^1,\sigma^2)$. The Polyakov action depends on the geometrical objects and not on the way we describe them via our parameterization of the coordinates. In other words the resultant value of the functional does not depend on the choice of local coordinates.

Another important consideration is the choice of the embedding space and its geometry. In general, we need information about the task at hand in order to adopt the right geometry.

Using standard methods in the calculus of variations, the Euler-Lagrange (EL) equations, with respect to the embedding, are (see [10] for derivation):

$$-\frac{1}{2\sqrt{g}}h^{il}\frac{\delta S}{\delta X^l}=\frac{1}{\sqrt{g}}\partial_\mu(\sqrt{g}g^{\mu\nu}\partial_\nu X^i)+\Gamma^i_{jk}\partial_\mu X^j\partial_\nu X^k g^{\mu\nu}, \tag{8}$$

where Γ^i_{jk} are the Levi-Civita connection coefficients with respect to the metric h_{ij} (defined in Eq. (12)), that describes the geometry of the embedding space.

We view scale-space as the gradient descent:

$$X^i_t\equiv\frac{\partial X^i}{\partial t}=-\frac{1}{2\sqrt{g}}h^{il}\frac{\delta S}{\delta X^l}. \tag{9}$$

Note that we used our freedom to multiply the Euler-Lagrange equations by a strictly positive function and a positive definite matrix. This is done in order to get a reparameterization invariant expression. This choice guarantees that the flow is geometric and does not depend on the parameterization. The operator that is acting on X^i in the first term of Eq. (8) is the natural generalization of the Laplacian from flat spaces to manifolds, denoted by Δ_g and called the Laplace-Beltrami operator or in short *Beltrami operator*. When the embedding is in a Euclidean space with Cartesian coordinate system, the connection elements are zero. If the embedding space is not Euclidean, we have to include the Levi-Civita connection term since it is not identically zero any more.

4. THE BELTRAMI FLOW

The metric of the embedding space is composed of the spatial metric and the color space metric as a direct sum, namely:

$$ds^2=ds^2_{spatial}+\beta ds^2_{feature}. \tag{10}$$

More general line elements for the color-spatial space are, in principle, possible. One such possibility is to consider a non-constant β such that the strength of the conjugation between the spatial and color coordinates is fixed locally in space and/or the image colors. This possibility as well as the issue of how to choose β is dealt with elsewhere [12].

Other possibilities may include a non-trivial metric elements that tie together spatial and color coordinates (i.e. non trivial coefficients of $dxdI$ for grey level images, or $dydR$ for color images). These possibilities are not very well understood theoretically and their implications are under current investigation.

The color space metrics in Section 2 are all diagonal, namely have the form $h_{ij}=\beta\alpha_{ii}(R,G,B)\delta_{ij}$.

The induced metric elements are according to Eq. (6):

$$\begin{aligned}g_{11}&=1+\beta(\alpha_{rr}R_x^2+\alpha_{gg}G_x^2+\alpha_{bb}B_x^2)\\ g_{12}&=g_{21}=\beta(\alpha_{rr}R_xR_y+\alpha_{gg}G_xG_y+\alpha_{bb}B_xB_y)\\ g_{22}&=1+\beta(\alpha_{rr}R_y^2+\alpha_{gg}G_y^2+\alpha_{bb}B_y^2).\end{aligned} \tag{11}$$

Note also that this two-dimensional image induced metric is different from the one we had in the Euclidean case. This implies that the choice of the color space geometry has a direct impact on the first term in the diffusion equation (i.e. $\frac{1}{\sqrt{g}}\partial_\mu(\sqrt{g}g^{\mu\nu}\partial_\nu X^i)$.) This is not the only place where changes should be made. The second term which includes the Levi-Civita connection coefficients, which are non-trivial in this case, should be evaluated as well. The definition of the Levi-Civita coefficients is

$$\Gamma^i_{jk}=\frac{1}{2}h^{il}(\partial_j h_{lk}+\partial_k h_{jl}-\partial_l h_{jk}), \tag{12}$$

where there is an implicit sum over l.

In the case of the Schrödinger model we find, for example:

$$\alpha_{ii}=\frac{1}{LI_i}, \tag{13}$$

where $L=c_rR+c_gG+c_bB$. A short analysis results in the following coefficients

$$\Gamma^i_{jk}=\frac{c_jI_i}{2LI_j}\delta_{jk}-\frac{c_j}{2L}\delta_{ik}-\frac{c_k}{2L}\delta_{ij}-\frac{1}{2I_i}\delta_{ij}\delta_{ik}. \tag{14}$$

Combining Eqs. (8)(11) and (14) together we finally get the following flow:

$$\begin{aligned}R_t&=\Delta_gR\\ &-(\frac{1}{2R}+\frac{c_r}{2L})(R_x^2g^{11}+2R_xR_yg^{12}+R_y^2g^{22})\\ &-\frac{c_g}{L}(R_xG_xg^{11}+(R_xG_y+R_yG_x)g^{12}+R_yG_yg^{22})\\ &-\frac{c_b}{L}(R_xB_xg^{11}+(R_xB_y+R_yB_x)g^{12}+R_yB_yg^{22})\\ &+\frac{c_gR}{2LG}(G_x^2g^{11}+2G_xG_yg^{12}+G_y^2g^{22})\\ &+\frac{c_bR}{2LB}(B_x^2g^{11}+2B_xG_yg^{12}+B_y^2g^{22})\end{aligned} \tag{15}$$

where

$$\begin{aligned}\Delta_gR=&\left(\frac{g_xg^{11}}{2g}+\frac{g_yg^{12}}{2g}+g^{11}_x+g^{12}_y\right)R_x+\\ &\left(\frac{g_xg^{12}}{2g}+\frac{g_yg^{22}}{2g}+g^{12}_x+g^{22}_y\right)R_y+\\ &g^{11}R_{xx}+2g^{12}R_{xy}+g^{22}R_{yy}.\end{aligned} \tag{16}$$

Here $g^{ij}_x=\partial g^{ij}/\partial x$ ($g^{ij}_y=\partial g^{ij}/\partial y$) and $g_x=\partial g/\partial x$ ($g_y=\partial g/\partial y$).

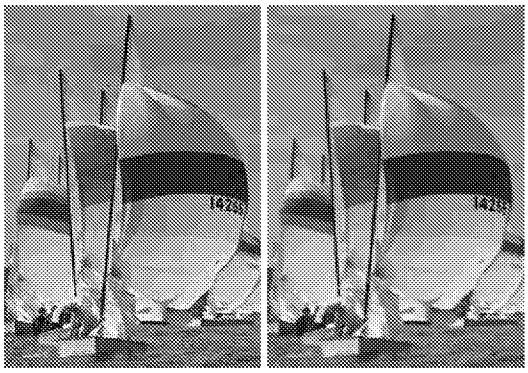

Figure 1: The sailboats image constructed from a CCD camera by a de-mosaicing algorithm. Left: Original image. Right: Stiles with $\beta = 1$. (this is a color image)

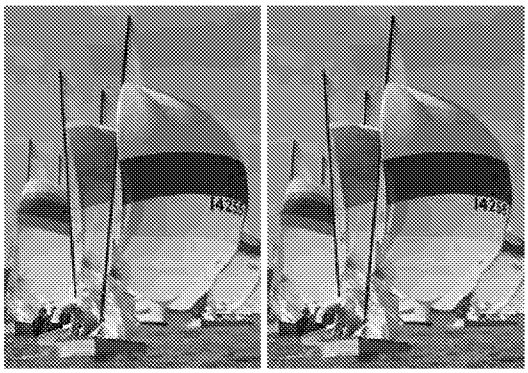

Figure 2: Left: Stiles with $\beta = 5$, Right: Schrödinger algorithm. (for a closer look point to http://www-ee.technion.ac.il/users/zeevi/zeevi.htm)

Other models are calculated similarly. The application of these models results in the images presented in Figs. (1) and (2). The processing is executed by the Euler approximation of the PDE, with central difference scheme for the spatial derivatives and backward scheme for the time derivative.

These images illustrate profound differences between the effects of the various smoothing schemes. However, quantative comparison is difficult since there is no universal quality criterion. A detailed comparison according to different classes of images and quality measures remains to be done.

5. REFERENCES

[1] G. Buchsbaum and A. Gottschalk. Trichrmacy, opponent colors coding and optimum color information transmission in the retina. *Proc. Roy. Soc. London Ser. B*, 220:89–113, 1983.

[2] H Helmholtz von. *Handbuch der Psychologishen Optik*. Voss, Hamburg, 1896.

[3] R. Kimmel R. Malladi and N. Sochen. Images as embedded maps and minimal surfaces: Movies, color, texture, and volumetric medical images. LBNL ,UC and TAUHEP Report LBNL-40490, UC-405, June 1997.

[4] Koenderink et al. *Kibernetik*, 6:227–237, 1970.

[5] D L MacAdam. Visual sensitivity to color differences in daylight. *J. Opt. Soc. Am.*, 32:247, 1942.

[6] D L MacAdam. Specification of small chromaticity differences. *J. Opt. Soc. Am.*, 33:18, 1943.

[7] A M Polyakov. Quantum geometry of bosonic strings. *Physics Letters B*, 103B(3):207–210, 1981.

[8] E Schrödinger. Grundlinien einer theorie der farbenmetrik in tagessehen. *Ann. Physik*, 63:481, 1920.

[9] N. Sochen, R. Kimmel, and R. Malladi. From high energy physics to low level vision. Report LBNL 39243, LBNL, UC Berkeley, CA 94720, August 1996.

[10] N. Sochen R. Kimmel and R. Malladi. A general framework for low level vision. *IEEE Trans. IP*, 7:310, 1997.

[11] N. Sochen and Y.Y. Zeevi. Images as Manifolds Embedded in a Feature-Spatial Non-Euclidean Space *in preparation*, 1998.

[12] N. Sochen and Y.Y. Zeevi. Representation of Colored Images by Manifolds Embedded in Higher Dimensional Non-Euclidean Space *ICIP98*, 1998.

[13] W S Stiles. A modified Helmholtz line element in brightness-color space. *Proc. Phys. Soc. (London)*, 58:41, 1946.

[14] J J Vos and P L Walraven. An analytical description of the line element in the zone-fluctuation model of color vision II. The derivative of the line element. *Vision Research*, 12:1345–1365, 1972.

[15] S Wolf R Ginosar and Y. Y. Zeevi. Spatio-Chromatic image enhancement based on a model of human visual information processing. *J. Vis. Com. Im. Rep.*. 9:25–37, 1998.

[16] G Wyszecki and W S Stiles. *Color Science: Concepts and Methods, Qualitative Data and Formulae, (2nd edition)*. John Wiley & Sons, 1982.